Destructive Interference in the Electron Tunneling through Protein Media

Tsutomu Kawatsu,[†] Toshiaki Kakitani,* and Takahisa Yamato

Department of Physics, Graduate School of Science, Nagoya University, Chikusa-ku, Nagoya 464-8602, Japan

Received: April 29, 2002; In Final Form: August 10, 2002

We investigated the origin of the very rapid and large fluctuation of the electron tunneling matrix element T_{DA} due to the thermal fluctuation of protein conformation which was recently observed by the simulation study (Daizadeh, I.; Medvedev, E. S.; Stuchebrukhov, A. A. *Proc. Natl. Acad. Sci. U.S.A.* **1997**, *94*, 3703). We made analysis of this phenomena by using the interatomic tunneling current map of Ru-modified azurins. We defined a new index, degree of destructive interference Q, by making an average of the intermediate level for the interatomic tunneling currents. We found an empirical relation that $|T_{DA}|$ is proportional to Q^{-1} holds true in the course of thermal fluctuation of protein conformation. Comparing maps of the interatomic tunneling currents with different values of Q, we found that the very rapid (in much less than 1 ps) and large amount (maximally 2 orders of magnitude) of fluctuations in T_{DA} are caused by the reconnection and the change in the direction of interatomic tunneling currents with considerable amplitudes. By taking the statistical average for the dynamics effect of log $|T_{DA}|$, we found that the range of the averaged dynamic modification of electron transfer rate amounts to more than 2 orders of magnitude in the Ru-modified azurins. In the systems with a large range of dynamic modification, this nuclear dynamics effect contributes to enhance the thermally averaged electron transfer rate considerably.

1. Introduction

The long-range electron transfer in proteins plays a significant role in biological energy conversions. Such electron transfer rate is expressed by a product of two factors: the electronic factor (square of the electron tunneling matrix element T_{DA}) and the nuclear factor (Franck−Condon factor).[1] This tunneling matrix element is evaluated by the superexchange mechanism through protein environments. It has long been believed that the nuclear factor is strongly dependent on the thermal fluctuation of protein conformations called nuclear dynamics but that the electronic factor will not be significantly dependent on the nuclear dynamics. However, recently Stuchebrukhov and coworkers found that T_{DA} can vary considerably within a time range of picoseconds depending on the protein conformation of Ru-modified azurin[2] and a molecular complex containing $FADH^-$, DNA, and DNA photolyase[3] under thermal fluctuation. The similar large fluctuation of T_{DA} was also found in the electron transfer through oligopeptides[4] and the electron transfer from cytochrome c_2 to the special pair of the photosynthetic reaction center.[5] The origin of such large and rapid variation of T_{DA} is a challenging problem to be solved at the present time.

Balabin and Onuchic have examined the effects of the protein nuclear dynamics on the electron tunneling matrix element in the bacterial photosynthetic reaction center.[6] They conducted the MD simulation for a part of the reaction center. They calculated the "coherence parameter" $C = \langle T_{DA}\rangle^2/\langle T_{DA}^2\rangle$, which measures how much degree the thermal average of T_{DA} remains the same during the thermal fluctuation, where "$\langle\ \rangle$" expresses an average of time steps of the MD simulation. They evaluated T_{DA} on the basis of the "tube model" [7−9] which is an advanced version of the "pathway model".[10,11] They made use of this coherence parameter as follows. When the value of C is close to 1, T_{DA} is nearly constant among various protein conformations, and it is almost independent of the nuclear dynamics as expected before. In contrast to this, when the value of C is close to 0, T_{DA} sharply fluctuates with the protein conformations. Namely, the electronic factor is strongly dependent on the nuclear dynamics. They found that this latter case applies to the electron transfer from the primary quinone Q_A to the secondary quinone Q_B. In this case, it is expected that the tunneling is controlled by the effect of cancellation among the contributions from the tunneling tubes.[12]

An advantage of the tube model is to make the physical meaning of the coherence parameter clear. The electron tunneling matrix element T_{DA} is expressed as a sum of $t_{DA}(i)$ which is the electron tunneling matrix element calculated by the ith tube. The $t_{DA}(i)$ has a sign as a phase factor. Then, tubes are classified into two groups with reference to the sign. When T_{DA} is positive, for example, the tubes with positive $t_{DA}(i)$ are considered to form "constructive interference" among them, and the tubes with negative $t_{DA}(i)$ are considered to play a role of "destructive interference" with the tubes with positive $t_{DA}(i)$.[6] When T_{DA} is negative, the tubes with negative $t_{DA}(i)$ form constructive interference and the tubes with positive $t_{DA}(i)$ play a role of destructive interference. On the basis of this consideration, one can expect that T_{DA} becomes large when the constructive interferences predominate and it becomes small when the destructive interferences work significantly.

Here, it should be mentioned that the importance of the phase relation among the electronic states of donor, mediator, and acceptor has been much discussed in the intramolecular long-distance electron transfer.[13−16] The effect of the configurational geometry of the mediator was also investigated in much detail by Paddon-Row.[13]

The problem, however, that arises is how much the tube model is appropriate for describing the interference problem. It

* To whom correspondence should be addressed. E-mail: kakitani@allegro.phys.nagoya-u.ac.jp.

[†] Present address: Department of Chemistry, Box 90349, Duke University, Durham, NC 27708-0346.

10.1021/jp026035y CCC: $22.00
Published on Web 10/03/2002

is well recognized that the tube model works nicely for the description of the global feature of the tunneling route.[7−9] So far, no detailed examination on the validity of the tube model for the phase problem has been made. The electron tunneling through a tube is independent from each other. Namely, electron tunnelings among the tubes are neglected. However, it appears that this is not the case in the Ru-modified azurins in which much detailed analysis of the electron tunneling route was made recently, based on the description of interatomic tunneling currents.[17,18] Namely, the interatomic tunneling currents connected many atoms, forming a web of tunneling pathways, and its separation into tubes appears to be almost impossible. Therefore, a more advanced method than the tube model should be devised for the investigation of the coherent phase effect in the tunneling process.

In our previous work,[17,18] we developed a novel method for determining the electron tunneling route, using the interatomic electron tunneling currents the treatment of which was much developed by Stuchebrukhov.[19−22] A set of the calculated interatomic tunneling currents involves all of the effects of the interferences in the electron tunneling matrix element T_{DA}.[17,18] We showed that a global picture of space-averaged interatomic currents becomes a simple form which looks like a worm.[18] Therefore, the interatomic tunneling current map has an advantage over the tube model for investigating the coherent phase effect in the overall tunneling process. In this paper, we define a new index "degree of destructive interference" Q which is calculable using the interatomic tunneling currents. We show that this index is quite useful for abstracting an essence of the interference effects among various interatomic tunneling currents. We shall demonstrate that $|T_{DA}|$ is inversely proportional to the degree of destructive interference by numerical calculations for Ru-modified azurins. We also propose another index D measuring the range of the averaged dynamic modification for the electron transfer rate.

In section 2, we write down basic equations for the electron tunneling in protein media which are necessary for the discussion in the latter section. In section 3, we explain the method of the MD simulation and the method of calculation of the electronic state as well as the definition of the electron transfer system. In section 4, results of numerical calculations are shown. In section 5, we discuss the origin of the rapid and large amplitude of fluctuation of $|T_{DA}|$ with reference to the destructive interference effect. The last section is contributed to conclusions.

2. Basic Equations for the Electron Tunneling

We derive some basic equations of electron tunnelings through protein environments which are used in the present paper. The rate of the long-range electron transfer is usually expressed by Marcus theory[1] in which the Condon approximation and the Fermi's golden rule are used:

$$k_{ET} = \frac{2\pi}{\hbar}|T_{DA}|^2(\mathrm{FC}) \tag{1}$$

where T_{DA} is the electron tunneling matrix element, and (FC) is the Franck−Condon factor. Usually, $|T_{DA}|^2$ is called the electronic factor. Based on the Born−Oppenheimer approximation, this equation can be rewritten more generally as follows

$$k_{ET} = \left\langle \frac{2\pi}{\hbar}\sum_{E_{fv}} \left| \langle \Psi_{iu}(\boldsymbol{r},\boldsymbol{R})|\hat{T}^{DA}|\Psi_{fv}(\boldsymbol{r},\boldsymbol{R})\rangle_{\boldsymbol{r},\boldsymbol{R}} \right|^2 \delta(E_{iu} - E_{fv}) \right\rangle_{E_{iu}} \tag{2}$$

where Ψ_{iu} and Ψ_{fv} are the vibronic wave functions in the initial and final states. The coordinates $\boldsymbol{r}$ and $\boldsymbol{R}$ are positions for electrons and nuclei. The $\hat{T}^{DA}$ is the electron tunneling operator. The bracket $\langle\ \rangle_{E_{iu}}$ is the thermal average over the vibronic state iu, the bracket $\langle\ \rangle_{\boldsymbol{r},\boldsymbol{R}}$ indicates the integral over $\boldsymbol{r}$ and $\boldsymbol{R}$, and E_{iu} and E_{fv} are the energies of the vibronic states iu and fv, respectively. The vibronic wave functions can be written as

$$\Psi_{iu}(\boldsymbol{r},\boldsymbol{R}) = \psi_i(\boldsymbol{r},\boldsymbol{R})\chi_{iu}(\boldsymbol{R}) \tag{3}$$

$$\Psi_{fv}(\boldsymbol{r},\boldsymbol{R}) = \psi_f(\boldsymbol{r},\boldsymbol{R})\chi_{fv}(\boldsymbol{R}) \tag{4}$$

where $\psi_i(\boldsymbol{r},\boldsymbol{R})$ and $\psi_f(\boldsymbol{r},\boldsymbol{R})$ are the electronic wave functions in the initial and final states, which include the nuclear coordinate as a parameter, and $\chi_{iu}(\boldsymbol{R})$ and $\chi_{fv}(\boldsymbol{R})$ are the vibrational wave functions in the vibronic states iu and fv, respectively. Substituting eqs 3 and 4 into eq 2, we obtain

$$k_{ET} = \left\langle \frac{2\pi}{\hbar}\sum_{E_{fv}} \left| \langle T_{DA}(\boldsymbol{R})\chi_{iu}(\boldsymbol{R})\chi_{fv}(\boldsymbol{R})\rangle_{\boldsymbol{R}} \right|^2 \delta(E_{iu} - E_{fv}) \right\rangle_{E_{iu}} \tag{5}$$

where

$$T_{DA}(\boldsymbol{R}) = \langle \psi_i(\boldsymbol{r},\boldsymbol{R})|\ \hat{T}^{DA}|\psi_f(\boldsymbol{r},\boldsymbol{R})\rangle_{\boldsymbol{r}} \tag{6}$$

In such a representation, the electron tunneling matrix element $T_{DA}(\boldsymbol{R})$ is a function of the vibrational coordinate, especially of the protein conformation coordinates. In the following, however, we express $T_{DA}(\boldsymbol{R})$ as T_{DA} for simplicity although we reserve the $\boldsymbol{R}$-dependence of T_{DA}.

A basic formula of T_{DA} was given by Larsson[23,24] for the first time. Later, this theory was reformulated,[9−11] and finally, it was expressed by the pseudo-Greens' function.[34,35] In the following, we introduce the method of calculating T_{DA}[25−31] and interatomic tunneling currents[19−22] using this advanced method.

Now, we suppose a system that the tunneling electron almost exists at the donor (D) in the initial state and at the acceptor (A) in the final state. Then, the molecular orbitals in the initial and final states are given as

$$\psi^i = C_D^i\phi_D + \sum_\nu C_\nu^i\phi_\nu \tag{7}$$

$$\psi^f = C_A^f\phi_A + \sum_\nu C_\nu^f\phi_\nu \tag{8}$$

where ϕ_D and ϕ_A are the molecular orbitals of the donor and acceptor, respectively. ϕ_ν is the atomic orbital included in the mediator. Here, we have assumed that the functional forms of ϕ_D and ϕ_A are not changed by the interaction with the mediator. The energies of the initial and final states are

$$E_i = \frac{\langle\psi^i|H|\psi^i\rangle}{\langle\psi^i|\psi^i\rangle} \tag{9}$$

$$E_f = \frac{\langle\psi^f|H|\psi^f\rangle}{\langle\psi^f|\psi^f\rangle} \tag{10}$$

where H is the one-electron Hamiltonian in our system. At the stationary state, following equations should be satisfied:

$$\frac{\partial E_i}{\partial C_\nu^i} = 0, \quad \frac{\partial E_f}{\partial C_\nu^f} = 0. \tag{11}$$

Substituting eq 11 into eqs 9 and 10, we obtain the following secular equations

$$C_{\mathrm{D}}^{\mathrm{i}}(H_{\mathrm{D}\nu} - E_{\mathrm{i}}S_{\mathrm{D}\nu}) + \sum_{\mu} C_{\mu}^{\mathrm{i}}(H_{\nu\mu} - E_{\mathrm{i}}S_{\nu\mu}) = 0, \tag{12}$$

$$C_{\mathrm{A}}^{\mathrm{f}}(H_{\nu\mathrm{A}} - E_{\mathrm{f}}S_{\nu\mathrm{A}}) + \sum_{\mu} C_{\mu}^{\mathrm{f}}(H_{\nu\mu} - E_{\mathrm{f}}S_{\nu\mu}) = 0, \quad (\nu = 1, 2, ...) \tag{13}$$

where

$$H_{\mathrm{D}\nu} = \langle\phi_{\mathrm{D}}|H|\phi_{\nu}\rangle \tag{14}$$

$$H_{\nu\mathrm{A}} = \langle\phi_{\nu}|H|\phi_{\mathrm{A}}\rangle \tag{15}$$

$$H_{\nu\mu} = \langle\phi_{\nu}|H|\phi_{\mu}\rangle \tag{16}$$

$$S_{\mathrm{D}\nu} = \langle\phi_{\mathrm{D}}|\phi_{\nu}\rangle \tag{17}$$

$$S_{\nu\mathrm{A}} = \langle\phi_{\nu}|\phi_{\mathrm{A}}\rangle \tag{18}$$

$$S_{\nu\mu} = \langle\phi_{\nu}|\phi_{\mu}\rangle \tag{19}$$

When the electron tunneling takes place, $E_{\mathrm{i}} = E_{\mathrm{f}} \equiv E$ is satisfied. We define some matrixes

$$(1/G)_{\mu\nu} \equiv ES_{\mu\nu} - H_{\mu\nu} \tag{20}$$

$$D_{\mu}^{\dagger} \equiv ES_{\mathrm{D}\mu} - H_{\mathrm{D}\mu} \tag{21}$$

$$A_{\nu} \equiv ES_{\nu\mathrm{A}} - H_{\nu\mathrm{A}} \tag{22}$$

Here, it should be noticed that the above $\boldsymbol{G}$ is different from the true Greens' function $\boldsymbol{S}(E\boldsymbol{S} - \boldsymbol{H})^{-1}\boldsymbol{S}$.[27] Substituting eqs 20−22 into eqs 12 and 13 and solving the coupled equations, we obtain[25,26]

$$C_{\nu}^{\mathrm{i}} = -C_{\mathrm{D}}^{\mathrm{i}}\sum_{\mu} D_{\mu}^{\dagger}G_{\mu\nu}\Big/\sqrt{\mathrm{Pop}^{\mathrm{i}}} \tag{23}$$

$$C_{\nu}^{\mathrm{f}} = -C_{\mathrm{A}}^{\mathrm{f}}\sum_{\mu} G_{\nu\mu}A_{\mu}\Big/\sqrt{\mathrm{Pop}^{\mathrm{f}}} \tag{24}$$

where $(\mathrm{Pop}^{\mathrm{i}})^{1/2}$ and $(\mathrm{Pop}^{\mathrm{f}})^{1/2}$ are normalization factors[25] which are expressed as

$$\mathrm{Pop}^{\mathrm{i}} = \sum_{n,m\in\mathrm{all}} C_n^{\mathrm{i}}S_{nm}C_m^{\mathrm{i}} \tag{25}$$

$$= C_{\mathrm{D}}^{\mathrm{i}\,2} + 2C_{\mathrm{D}}^{\mathrm{i}}\sum_{\mu} C_{\mu}^{\mathrm{i}}\,S_{\mathrm{D}\mu} + \sum_{\mu\nu} C_{\mu}^{\mathrm{i}}\,C_{\nu}^{\mathrm{i}}S_{\mu\nu} \tag{26}$$

$$\mathrm{Pop}^{\mathrm{f}} = \sum_{n,\,m\in\mathrm{all}} C_n^{\mathrm{f}}S_{nm}C_m^{\mathrm{f}} \tag{27}$$

$$= C_{\mathrm{A}}^{\mathrm{f}\,2} + 2C_{\mathrm{A}}^{\mathrm{f}}\sum_{\mu} C_{\mu}^{\mathrm{f}}S_{\mathrm{A}\mu} + \sum_{\mu\nu} C_{\mu}^{\mathrm{f}}\,C_{\nu}^{\mathrm{f}}S_{\mu\nu} \tag{28}$$

Then, the total tunneling matrix element T_{DA} is given as follows:[25]

$$T_{\mathrm{DA}} = \langle\psi^{\mathrm{i}}|\,E\hat{I} - \hat{H}|\psi^{\mathrm{f}}\rangle \tag{29}$$

$$= \sum_{\mu\nu} C_{\mu}^{\mathrm{i}}(ES - H)_{\mu\nu}C_{\nu}^{\mathrm{f}} \tag{30}$$

$$= \frac{\sum_{\mu\nu} D_{\mu}^{\dagger}G_{\mu\nu}A_{\nu}}{\sqrt{\mathrm{pop}^{\mathrm{i}}}\sqrt{\mathrm{pop}^{\mathrm{f}}}} \tag{31}$$

with

$$\mathrm{pop}^{\mathrm{i}} = \frac{\mathrm{Pop}^{\mathrm{i}}}{C_{\mathrm{D}}^{\mathrm{i}\,2}} \tag{32}$$

$$\mathrm{pop}^{\mathrm{f}} = \frac{\mathrm{Pop}^{\mathrm{f}}}{C_{\mathrm{D}}^{\mathrm{f}\,2}} \tag{33}$$

In the above treatment, a direct interaction between the donor and acceptor is ignored. Usually, the factor $1/[(\mathrm{pop}^{\mathrm{i}})^{1/2}(\mathrm{pop}^{\mathrm{f}})^{1/2}]$ is approximated as 1 because the coupling between donor and mediator and the coupling between acceptor and mediator are considered to be small.[32−36] However, this factor cannot be put as 1 in the case of the intermolecular electron transfer where donor and acceptor are linked by the chemical bonds or in the case of the electron transfer in protein environment where donor or acceptor is strongly coupled with the ligand.[25] It was discussed by Larsson[37] that the strong coupling effect appears in the spectral shift in a blue copper protein.

The electron tunneling current $J_{\mu\nu}(t)$ between the atomic orbital μ and ν which is derived in the appendix by a method a little different from that of Stuchebrukhov[19−22] is written as follows:

$$J_{\mu\nu}(t) = \frac{1}{\hbar}(C_{\mu}^{\mathrm{i}}\,C_{\nu}^{\mathrm{f}} - C_{\mu}^{\mathrm{f}}\,C_{\nu}^{\mathrm{i}})(H_{\mu\nu} - ES_{\mu\nu})\,\sin(2\omega t) \tag{34}$$

where $\omega = T_{\mathrm{DA}}/\hbar$. The oscillatory time-dependent part $\sin(2\omega t)$ is common to all of the tunneling currents. Then, we use the part of the time-independent tunneling current:

$$J_{\mu\nu} = \frac{1}{\hbar}(C_{\mu}^{\mathrm{i}}\,C_{\nu}^{\mathrm{f}} - C_{\mu}^{\mathrm{f}}\,C_{\nu}^{\mathrm{i}})(H_{\mu\nu} - ES_{\mu\nu}) \tag{35}$$

An interatomic tunneling current is obtained as follows:

$$J_{\mathrm{ab}} = \sum_{\mu\in a,\nu\in b} J_{\mu\nu} \tag{36}$$

where a and b indicate atoms. The electron tunneling matrix element T_{DA} is expressed by using this interatomic tunneling current as follows:

$$\sum_{a\in\Omega_{\mathrm{D}}^{j},b\notin\Omega_{\mathrm{D}}^{j}} J_{ab} = \frac{1}{\hbar}T_{\mathrm{DA}} \tag{37}$$

where Ω_{D}^{j} is a region of the donor side from the plane j placed perpendicularly to the line connecting donor and acceptor. The value of the sum in eq 37 is independent of the position of the plane. This T_{DA} corresponds to $T_{\mathrm{DA}}^{\mathrm{nor}}$ in ref 25.

3. Method of Calculations

The MD simulation is conducted for collecting the protein conformations under thermal fluctuations. The molecular systems which we consider in this study are spherical vessels whose radii are 30 Å involving a protein (Ru-modified azurin) at its center and ca. 3000 water molecules surrounding the protein. The system is kept at the temperature of 300K. Electric fields from far atoms over distance 9 Å are approximated by the PPPC method.[38] The MD program PRESTO[39] is used with AMBER[40] force field together with metal force field set.[41,42] The MD step size is 1 fs, and the step size for the calculation of electron tunneling property is 100 fs in most cases.

We choose Ru-modified azurin for our electron transfer system. It is the system experimentally well investigated by performing various mutations for the protein. When it is exposed to light, the following reaction takes place:[43−46]

$$\mathrm{Cu(II)Ru(II)}^* \rightarrow \mathrm{Cu(I)Ru(III)(photo\text{-}induced\ charge\ separation)} \quad (38)$$

$$\mathrm{Cu(II)Ru(II)} \leftarrow \mathrm{Cu(I)Ru(III)(charge\ recombination)} \quad (39)$$

In the experiment, the rate of the charge recombination is measured.[43−46] The ruthenium complex ligates to the histidine residue. So, histidine mutants planted at various site of azurin provide various redox systems. This systematically produced system has a nice property that the same type of the donor−acceptor pair is placed with different distances and in various kinds of protein environments. In our computational calculations, the initial coordinates of the azurin structure are obtained from "1VLX" [47−49] in Protein Data Bank, and the Ru-complex coordinate is obtained from the work by Adman et al.[50] We investigated the tuneling property of the electron transfer in His83 (native), His107, His109, His122, His124, and His126 mutants experimentally produced by the Gray's group.[43−46]

We calculate the electron tunneling matrix element T_{DA} and electron tunneling currents J_{ab} by an extended Hückel level program as before.[17,18] We refer to the FORTICON8 program for the extended Hückel program[51] and some Hückel parameters by Vela's work.[52] Then, we use a ITPACK 2C[53] package for solving the secular equations. We have chosen the tunneling energy at −10.7 eV in all of the cases. This is a standard value in this molecular system.[17,18] We treated both of the protein and water molecules as electron tunneling mediators.

4. Results

4.1. Effect of Thermal Fluctuation on the Electron Tunneling Matrix Element. In this section, we demonstrate a big effect of the thermal fluctuation of the protein conformations (nuclear dynamics) on the electronic factor of the electron-transfer rate k_{ET}. First, we conduct MD simulations for the Ru-modified azurin systems and collect protein comformations under thermal fluctuations. Then, the electron tunneling matrix element T_{DA} is calculated for each conformation.

In Figure 1, we show how $|T_{DA}|$ and the distance between donor and acceptor fluctuate for the different protein conformations of the 6 kinds of azurin derivatives. Here, it should be noticed that the data points are plotted for the conformation at every 100 fs (totally 100 points for each derivative). We see sharp fluctuations of $|T_{DA}|$ by 2−3 orders of magnitude in all of the derivatives. The donor−acceptor distance fluctuates by 2 Å at most within the time scale of 10 ps.

In Figure 2, we plotted the time dependence of the electron tunneling matrix element $|T_{DA}|$ in His83 derivative. The data points are plotted at every 100 fs as in Figure 1. We see a fluctuation of $|T_{DA}|$ within a period of 0.1−1 ps. In Figure 3, we plotted $|T_{DA}|$ (top) and T_{DA} (bottom) for the His83 derivative at every 1 fs. We see fine random structures of fluctuation which take place in much less than 10 fs (sometimes in 1 fs). We also see a sharp dip in $|T_{DA}|$. The origin of this sharp dip in $|T_{DA}|$ is due to the crossing over the zero point in T_{DA}, as exemplified by the vertical dotted lines. Namely, we see no regular progression of peaks in $|T_{DA}|$ with period of 50−100 fs which was observed by Daizadeh et al.[2]

4.2. Degree of Destructive Interference *Q*. It is an interesting problem to analyze the mechanism by which rapid, large fluctuation of $|T_{DA}|$ is made possible under the small conformation charge of the protein environment. We notice the fact that the connectivity of the interatomic tunneling currents with large amplitude is not simple but is much complicated in many parts of the protein media. The manner of the connection might be neatly affected by a small change of the protein conformation. The direction of the interatomic tunneling current is another important factor for determining $|T_{DA}|$. We focus on the fluctuation of the connectivity and the direction of the interatomic tunneling currents with considerable amplitudes.

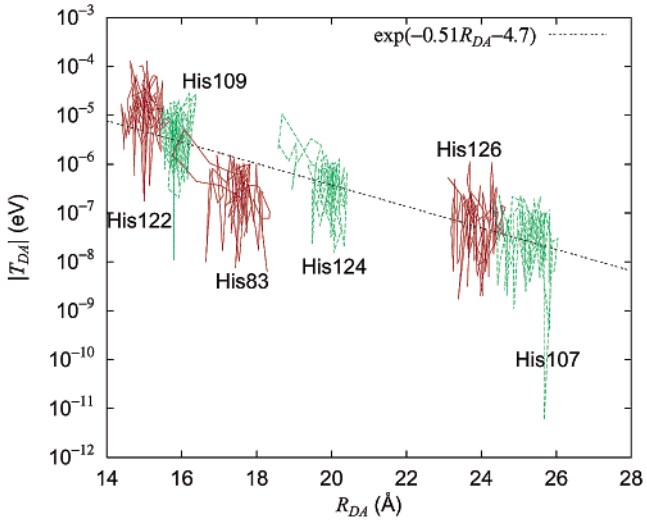

Figure 1. Plots of the electron tunneling matrix element $|T_{DA}|$ as a function of the donor−acceptor distance R_{DA} for the six kinds of Ru-modified azurins. Each point in the cluster is plotted at every 100 fs in the MD simulations Each cluster of points indicates an electron transfer in the derivative in His122, His109, His83, His124, His126 and His107 which are ligated by the ruthenium complex, respectively. The broken line indicates a fitting line for the centers of most clusters.

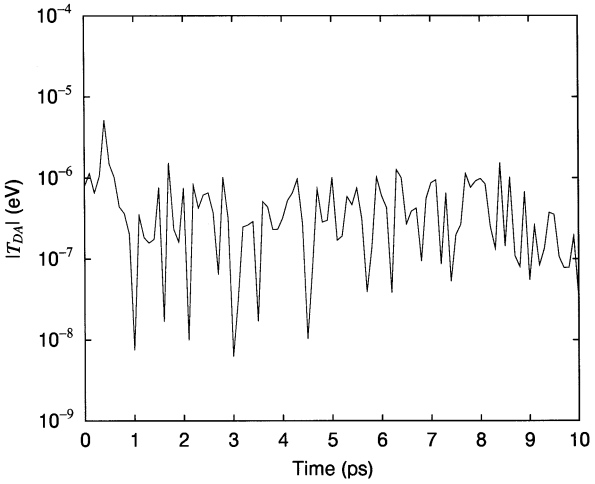

Figure 2. Time development of the calculated electron tunneling matrix element $|T_{DA}|$ for the Ru−His83. The $|T_{DA}|$ is calculated at every 100 fs of the MD simulation.

As we see in eq 37, the sum of the interatomic tunneling current J_{ab} through any plane is equal to the electron tunneling matrix element T_{DA} except a constant factor $\hbar$. Because J_{ab} has a sign, this sum is a vectorial sum scaled in one-dimensional space. Now, we make the sum of the absolute value of J_{ab} through a plane j as follows

$$\sum_{a\in\Omega_D^j}\sum_{b\notin\Omega_D^j}|J_{ab}| \equiv \frac{1}{\hbar}U_j \quad (40)$$

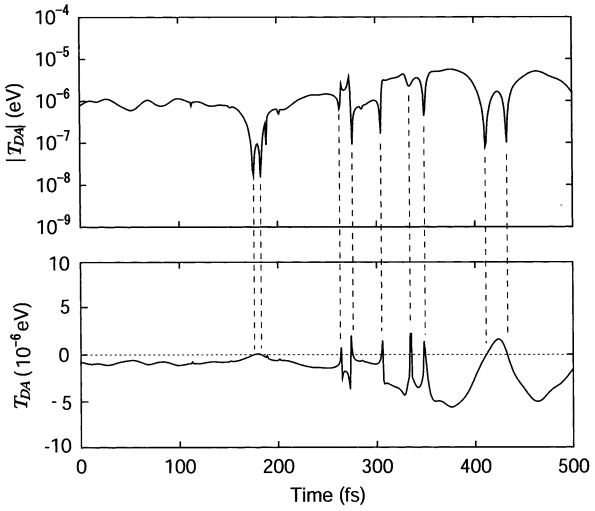

Figure 3. Detail of the time development of the calculated electron tunneling matrix element $|T_{DA}|$ and T_{DA} for Ru−His83 azurin. The $|T_{DA}|$ (top) and T_{DA} (bottom) are calculated at every 1 fs of the MD simulation.

In this case, U_j depends on the kind of plane j. This sum is the scalar sum. Then, we define Q_j as a ratio of U_j and $|T_{DA}|$ as follows:

$$Q_j \equiv \frac{U_j}{|T_{DA}|} = \frac{\sum_{a\in\Omega_D^j}\sum_{b\notin\Omega_D^j}|J_{ab}|}{\left|\sum_{a\in\Omega_D^j}\sum_{b\notin\Omega_D^j}J_{ab}\right|} \tag{41}$$

Physical meaning of Q_j is how many times the interatomic tunneling currents change their directions on the average in passing through the plane j. In other words, Q_j represents the effective number of changing the directions of the interatomic tunneling currents. This Q_j was defined before and its value was calculated as a function of the distance of plane j from donor in the His83 derivative.[18] In such calculations, Q_j varied considerably depending on the position of the plane j. Because these data describe too much detail of the tunneling current, we take average of Q_j over the whole plane j as follows:

$$Q \equiv \frac{1}{N}\sum_{j}^{N} Q_j \tag{42}$$

where N is total number of the planes between donor and acceptor. This Q is obtained for each conformation of the protein environment.

The value of Q is large when the effective number of changing directions of the interatomic tunneling currents is large. In this case, the tunneling currents do not flow smoothly from donor to acceptor, but they are suffered from much destructive interference. Therefore, Q should work as a nice index to measure how much the destructive interference takes place. Then, we call Q "degree of destructive interference".

We calculate the value of Q and the electron tunneling matrix element T_{DA} for various protein conformations produced by MD simulations for Ru-modified azurins. In Figure 4, we plotted 100 points of $|T_{DA}|$ as a function of Q which are calculated for the protein conformations at every 100 fs of His83 in Figure 1. We find that a nice correlation holds between $|T_{DA}|$ and Q. The broken line has a slope of -1, indicating that $|T_{DA}|$ is proportional to Q^{-1}. The data points fit nicely to this correlation line with some scattering. The similar data calculated for the

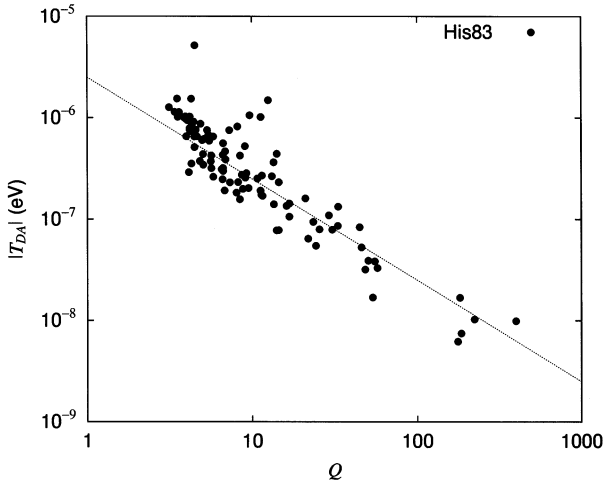

Figure 4. Correlation between the electron tunneling matrix element $|T_{DA}|$ and the degree of destructive interference Q. Each point is calculated at every 100 fs in the MD simulations of Ru−His83 azurin. The broken line represents a relation that $|T_{DA}|$ is proportional to Q^{-1}.

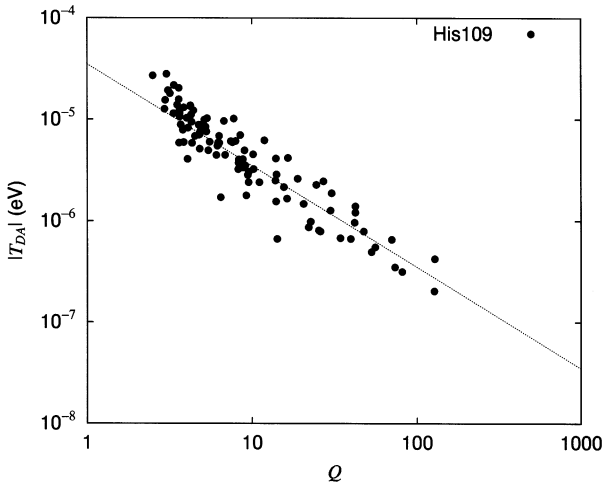

Figure 5. Correlation between the electron tunneling matrix element $|T_{DA}|$ and the degree of destructive interference Q. Each point is calculated at every 100 fs in the MD simulations of Ru−His109 azurin.

His109 derivative are plotted in Figure 5. We also see that $|T_{DA}|$ is linearly in good correlation with Q^{-1}. Such a relation was seen in all of the six derivatives which are investigated in this paper. Namely, we can summarize the above data by the following empirical formula:

$$|T_{DA}| = a\left(\frac{1}{Q}\right) \tag{43}$$

where a is a constant.

On the basis of these results, we conclude that the dominant factor by which $|T_{DA}|$ greatly fluctuates in a very short time scale is the variation of the degree of the destructive interference due to the fluctuation of protein conformation. When the degree of the destructive interference is large, $|T_{DA}|$ becomes small and vice versa.

4.3. Contribution of the Donor−Acceptor Distance Fluctuation. In Figure 1, we have shown that the distance R_{DA} between donor and acceptor fluctuates to some extent. Then, we try to subtract the effect of the distance from the fluctuation of $|T_{DA}|$ using a global dependence of the tunneling matrix element as expressed by a dotted line in Figure 1. Namely, we define a new tunneling matrix element T_{DA}^{*} as

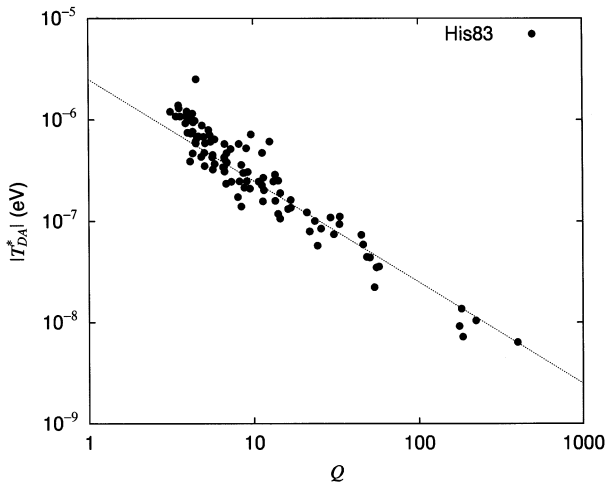

Figure 6. Correlation between the modified electron tunneling matrix element $|T^*_{DA}|$ and the degree of destructive interference Q. Each point is calculated at every 100 fs in the MD simulation of Ru−His83 azurin.

$$|T^*_{DA}| = |T_{DA}| \exp\{\alpha(R_{DA} - R_0)\} \tag{44}$$

with $\alpha = 0.5056$ Å^{-1} and $R_0 = 17.5$ Å. We use the value of R_{DA} obtained for each protein conformation under fluctuation.

In Figure 6, we plotted $|T^*_{DA}|$ as a function of Q for the His83 derivative. We find that the correlation between T^*_{DA} and Q is better than that between $|T_{DA}|$ and Q by decreasing the scattering width from a straight line. This straight line is the same between Figures 6 and 4. Therefore, we can say that the correlation of eq 43 holds regardless of the fluctuation of the donor−acceptor distance. The magnitude of the scattering of data points from the straight line in Figure 6 indicates a small residual effect which could not be included in averaging process of Q_j that varies with the position of the plane j.

5. Discussion

By the numerical calculations, we found that a nice correlation holds true between $|T_{DA}|$ and Q as shown in eq 42. This equation is similar to eq 41. Then, we take the average of U_j over the planes as follows

$$U \equiv \frac{1}{N}\sum_j U_j \tag{45}$$

Then, eq 42 reads

$$Q = \frac{U}{|T_{DA}|} \tag{46}$$

Comparing eq 46 with the empirical relation eq 43, we find that $U = a$ (constant) holds true for the variation of protein conformations due to the thermal fluctuation. Namely, we obtain the following relation:

$$\frac{1}{N}\sum_j \left(\sum_{a\in\Omega_D^j} \sum_{b\notin\Omega_D^j} |J_{ab}| \right) = a \text{ (constant)} \tag{47}$$

Let us consider the physical meaning of eq 47. Mathematically, the following relation must be satisfied:

$$\sum_{a\in\Omega_D^j} \sum_{b\notin\Omega_D^j} |J_{ab}| \geq \left| \sum_{a\in\Omega_D^j} \sum_{b\notin\Omega_D^j} J_{ab} \right| \equiv \frac{1}{\hbar}|T_{DA}| \tag{48}$$

The equality holds true when all of the signs of J_{ab} are same. In this case, U becomes $|T_{DA}|$, and Q becomes 1. This $|T_{DA}|$ is written as $|T^1_{DA}|$. Because eq 46 holds true for all of the cases of the fluctuation in protein conformation, we obtain

$$a = |T^1_{DA}| \tag{49}$$

Now, the conservation law in eq 47 shows that, even if the sign of J_{ab} may differ among various pairs of a and b, the sum of $|J_{ab}|$ remains the constant. This fact indicates that most of the absolute values of interatomic tunneling currents remain almost the same even if the sign of J_{ab} may change under the fluctuation of protein conformation. Therefore, when the signs of many interatomic tunneling currents passing through a plane are randomly distributed, the sum of J_{ab} (equivalently T_{DA}) becomes very small. On the other hand, when the signs of many interatomic tunneling currents passing through a plane are the same, the sum of J_{ab} (equivalently T_{DA}) becomes large. The signs of the interatomic tunneling currents with considerable amplitudes are easily changed by the fluctuation of protein conformation as we discuss in the latter part of this section. Therefore, these phase relations are the origin of the empirical relation of eq 46.

To exemplify the above qualitative argument by the interatomic tunneling current map, we define a new normalized interatomic tunneling current as follows:

$$\bar{K}_{ab} \equiv \frac{K_{ab}}{Q} = \hbar\frac{J_{ab}}{U} \tag{50}$$

where K_{ab} is the normalized interatomic tunneling current as defined previously[17]

$$K_{ab} = \hbar\frac{J_{ab}}{T_{DA}} \tag{51}$$

The advantage of K_{ab} is that it satisfies the sum rule

$$\sum_{a\in\Omega_D^j} \sum_{b\notin\Omega_D^j} K_{ab} = 1 \tag{52}$$

This property is quite useful for the discussion of the distribution of the normalized interatomic tunneling current for a given protein conformation. However, $|K_{ab}|$ becomes very large in the presence of much destructive interference (in the case of large Q) because the signs of K_{ab}'s are not uniform and the constraint of eq 52 applies. Therefore, the map of this interatomic tunneling current is not suitable to compare the distribution of tunneling currents with different values of Q. In contrast to this, the value of $|\bar{K}_{ab}|$ does not become much larger than 1, regardless of the values of Q. Therefore, the map of the new normalized interatomic tunneling current $\bar{K}_{ab}$ is suitable to compare the distribution of the tunneling currents with different values of Q.

Under such preparation, we have drawn the maps of $\bar{K}_{ab}$ in the case of $Q = 181.2$ as a typical case of large Q and in the case of $Q = 4.6$ as a typical case of small Q for His83 derivative in Figure 7. We find that the tunneling currents flow smoothly almost in the same direction in the case of $Q = 4.6$ but that the tunneling currents in the case of $Q = 181.2$ flow circularly and in a zigzag manner and also drop in the other parts than the route used in the case of $Q = 4.6$. This is the reconnection of the interatomic tunneling currents with considerable amplitude. In the case of $Q = 181.2$, the flow through the imidazole ring becomes a bottleneck. The connectivity and the direction of the

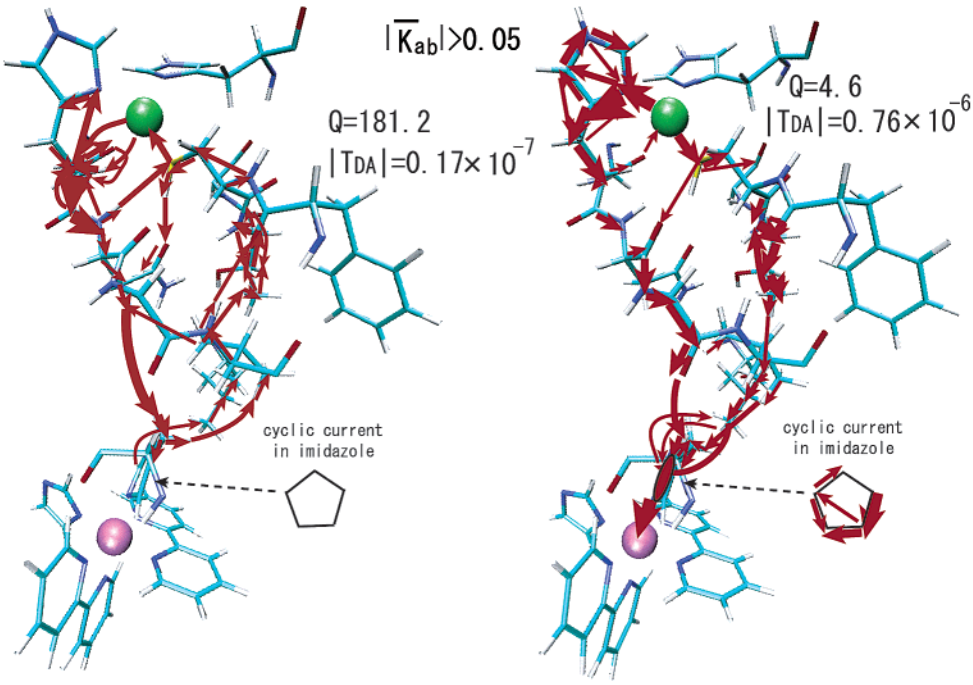

Figure 7. Maps of the newly defined normalized interatomic tunneling currents $\bar{K}_{ab}$ in the case of $Q = 181.2$ (left) and 4.6 (right) for Ru−His83 azurin. Only the interatomic tunneling currents with $|\bar{K}_{ab}| > 0.05$ are drawn.

interatomic tunneling currents differ very much between the maps of large Q and small Q. In the case of large Q, $|T_{DA}|$ is small (0.17×10^{-7} eV). In the case of small Q, $|T_{DA}|$ is large (0.76×10^{-6} eV). This connectivity and the direction of the interatomic tunneling current are determined by the phase relation among the interatomic tunneling currents passing through the atomic orbitals involved in the protein. Such phase relation is due to a pure coherent property in the tunneling phenomena. As a result, we conclude that the phase relation of the tunneling currents is very sensitive to the conformation of the protein environment. Such variation of the phase relation can cause a rapid and large amplitude of fluctuation in $|T_{DA}|$.

In the above analysis, we have disclosed a new fact that the signs and connectivity of the interatomic tunneling currents with considerable amplitudes are changed considerably by a short period of thermal fluctuation of the protein conformation. Then, why are the signs and connectivity of the interatomic tunneling currents so sensitive to the protein conformation? Combining eqs 35−37, we write

$$T_{DA} = \sum_{\mu \in \Omega_D^j} \sum_{\nu \notin \Omega_D^j} T_{\mu\nu} \tag{53}$$

$$T_{\mu\nu} = \hbar J_{\mu\nu} = (C_\mu^i C_\nu^f - C_\mu^f C_\nu^i)(H_{\mu\nu} - ES_{\mu\nu}) \tag{54}$$

where $T_{\mu\nu}$ is the tunneling matrix element contributed from the tunneling current from the atomic orbital μ to the atomic orbital ν. Let us make an order estimate of each factor: $H_{\mu\nu} - ES_{\mu\nu}$ is an order of 1 eV for neighboring atoms μ and ν. $T_{\mu\nu}$ is an order of 10^{-7} eV for the inter-orbital current with large amplitude in the case of His83 derivative. Then, $C_\mu^i C_\nu^f - C_\mu^f C_\nu^i$ is an order of 10^{-7}. Analyzing the calculated results, we found that $C_\mu^i C_\nu^f$ and $C_\mu^f C_\nu^i$ are mostly an order of 10^{-7}. Those molecular orbital coefficients can change their values and signs when the protein conformation is changed. Furthermore, it may happen for some protein conformations that $C_\mu^i C_\nu^f$ and $C_\mu^f C_\nu^i$ may cancel to each other or even overcancel to reverse the sign of $T_{\mu\nu}$. A very rapid change (in less than a few fs) of T_{DA} in Figure 3 may correspond to such cancellation or overcancellation. A large scale of destructive interference is caused by the accumulative effect of the above factors. Namely, for some protein conformations, the values of the coefficients C_μ^i, C_ν^f, C_μ^f, and C_ν^i are changed considerably and concomitantly cancellation or overcancellation between $C_\mu^i C_\nu^f$ and $C_\mu^f C_\nu^i$ takes place in every place involving the chemical bond, hydrogen bond, and through-space, and then it causes reconnections and changes of the signs of the interatomic tunneling currents. This is exemplified in Figure 7.

TABLE 1: Calculated Values of the Coherent Parameter C and the Ratio $|\langle T_{DA}\rangle|/\langle|T_{DA}|\rangle$ for the Six Kinds of Ru-Modified Azurins[a]

derivative	$C = \|\langle T_{DA}\rangle\|^2/\langle T_{DA}^2\rangle$	$\|\langle T_{DA}\rangle\|/\langle\|T_{DA}\|\rangle$
His83	0.185	0.673
His107	0.000340	0.028
His109	0.118	0.649
His122	0.0305	0.298
His124	0.0407	0.272
His126	0.159	0.549

[a] The bracket $\langle\ \rangle$ denotes the average over the fluctuating protein conformation.

Now, let us look at our study from the standpoint of Balabin and Onuchic.[6] We calculated the coherence parameter C for the six kinds of Ru-modified azurins. The result is shown in Table 1. We find that all of the calculated coherence parameters are considerably less than 1. Therefore, all of the cases belong to the destructive interference according to the classification of Balabin and Onuchic.[6] In Table 1, we list the ratio $|\langle T_{DA}\rangle|/\langle|T_{DA}|\rangle$ for the six derivatives. We see that the ratio is much smaller than 1 in all of the cases, indicating that the sign of T_{DA} changes frequently with almost similar amplitude. It is also seen that the ratio of His109 derivative is extremely small. To see Table 1 in more detail, the coherence parameter of His83 derivative is larger than the others. The electron tunneling route in His83 derivative must cross β strands sometimes in order for the tunneling current to flow from donor to acceptor. Therefore, the tunneling route is composed of much more complicated

connections of the interatomic tunneling currents than the other derivatives. Even if so, the coherence parameter is larger than the others. This fact indicates that the problem of the coherence is very much delicate, and it is not safe to judge the coherent property simply on the base of the secondary structure of the protein. Indeed, the secondary structure of the protein does not change during the thermal fluctuations of the protein conformation.

Here, we should point out one more important role of the conformational fluctuation in T_{DA}. As we see in Figure 3, the value of T_{DA} is changed very quickly, almost in less than 10 fs, sometimes in 1 fs. The time scale of the rapid change of T_{DA} should be much smaller than the period of skeletal motion of the protein and also the conformational relaxation time in the course of the electron transfer. Furthermore, it does not appear that the high-frequency vibration of C−H stretchings (about a period of 10 fs) alone will induce such a large amount of fluctuation of T_{DA} and a large scale of destructive interference among interatomic tunneling currents.

The main result of the present study was the finding of the proportionality of $|T_{DA}(\boldsymbol{R})|$ with $1/Q$ (eq 43) where we write down the explicit dependence of T_{DA} on R. Namely, $|T_{DA}(\boldsymbol{R})|$ increases with the decrease of Q. The degree of the destructive interference Q takes the smallest value 1 when all of the destructive interferences are ceased. In this case, $|T_{DA}(\boldsymbol{R})|$ has an upper bound value $|T_{DA}^1|$ as shown in eq 49. We can say that $|T_{DA}(\boldsymbol{R})|$ becomes maximum when all of the destructive interferences are ceased at certain protein conformation. The existence of such a maximum value of $|T_{DA}(\boldsymbol{R})|$ does not consolidate with the idea that the variation of $|T_{DA}(\boldsymbol{R})|$ with the conformation fluctuation is caused by the phonon-modified inelastic mechanism with the harmonic approximation.[2] In this theory, $|T_{DA}(\boldsymbol{R})|$ was expressed by an exponential form as a function of $\boldsymbol{R}$. The coefficient in the exponent was related to the electron−phonon coupling parameter κ. It was shown that this coupling works through the nuclear factor and modifies the ordinary Franck−Condon factor.[2] It is necessary that κ should have a considerably large value so that this phonon-modified inelastic mechanism with harmonic approximation can significantly modify the ordinary Franck−Condon factor. However, the adoption of such a large value of κ is in contradiction with the existence of the upper bound of $T_{DA}(\boldsymbol{R})$ because the exponential function of $T_{DA}(\boldsymbol{R})$ will easily break such boundary condition. Even for a moderate value of κ, it is possible that the exponential form of $T_{DA}(\boldsymbol{R})$ exceeds the upper bound from certain value of $\boldsymbol{R}$.

Therefore, our simulation data suggest that the protein conformation fluctuation is not harmonic, and more importantly the protein conformation dependence of the tunneling matrix element $T_{DA}(\boldsymbol{R})$ cannot be expressed by a simple exponential form of $\boldsymbol{R}$, but it is the much complicated function of $\boldsymbol{R}$ which is only known by the simulation study. As we already stated, the time scale of the variation of $T_{DA}(\boldsymbol{R})$ is sometimes less than a few femtoseconds and it is much smaller than the time scale of protein conformation fluctuations. The reason the time scale of the variation of $T_{DA}(\boldsymbol{R})$ is smaller than that of protein conformation change is that the value of $T_{DA}(\boldsymbol{R})$ is mainly determined by a much delicate phase relation of the interatomic tunneling currents through the modification of the molecular orbital coefficients. This fact indicates that the variation of $T_{DA}(\boldsymbol{R})$ is not directly correlated with the energy exchange problem between the electron and phonon systems.

Because $\chi_{iu}(\boldsymbol{R})\chi_{fv}(\boldsymbol{R})$ is related to the energetics of the phonon system and $T_{DA}(\boldsymbol{R})$ is related to the phase correlation among interatomic tunneling currents which will be almost independent of the energetics of the phonon system, it will be reasonable to adopt the thermal average of $T_{DA}(\boldsymbol{R})$ and $\chi_{iu}(\boldsymbol{R})\chi_{fv}(\boldsymbol{R})$ in eq 5 independently from each other as follows:

$$k_{ET} = \frac{2\pi}{\hbar}\langle T_{DA}{}^2\rangle(\mathrm{FC}) \tag{55}$$

where (FC) is the ordinary Franck−Condon factor defined by

$$(\mathrm{FC}) = \Big\langle \sum_{E_{fv}} |\langle \chi_{iu}(\boldsymbol{R})\chi_{fv}(\boldsymbol{R})\rangle_{\boldsymbol{R}}|^2 \delta(E_{iu} - E_{fv})\Big\rangle_{E_{iu}} \tag{56}$$

and $\langle T_{DA}{}^2\rangle$ is the thermally averaged electronic factor. Namely, the dynamical effect on the electronic factor would be approximately expressed by the average over the fluctuating protein conformations independently from the nuclear factor (FC). In the expression of eq 55, the inelastic effect is no more involved. The transient inelastic effect is retained in the electronic factor $\langle T_{DA}{}^2\rangle$.

Now, we proceed to measure the nuclear dynamical effect on the electronic factor more quantitatively. In Figures 4 and 5, we find that $|T_{DA}|$ varies within a range of almost 2 orders of magnitude. Considering this fact, we calculate the average of log $|T_{DA}|$ and then the standard deviation σ for the distribution of log $|T_{DA}|$ as follows:

$$\sigma = \sqrt{\langle(\log |T_{DA}|)^2\rangle - \langle \log |T_{DA}|\rangle^2} \tag{57}$$

Then, we evaluate the "range of the averaged dynamic modification" D for the electronic factor $|T_{DA}|^2$ which is defined as follows:

$$D \equiv (10^{2\sigma})^2 = 10^{4\sigma} \tag{58}$$

The calculated results of σ and D for the six derivatives are listed in Table 2. We see that the range of the averaged dynamic modification is a little larger than 2 orders of magnitude. This is a moderate estimate of the range if we look at the large variation of $|T_{DA}|^2$ which ranges mostly 4 orders of magnitude as calculated from Figure 4. The physical meaning of this range is as follows. For a single protein conformation, its $|T_{DA}|$ is one of the points in such as Figures 4 or 5. Even if its conformation is chosen to be that determined by the crystallographic study, its value of $|T_{DA}|$ cannot necessarily be the largest one but drops in some point in the above figure. In such a case, the range of the averaged dynamic modification gives a measure to see the region in which the point drops in. The thermally averaged electronic factor in eq 55 takes full account of the nuclear dynamic effect, and so it uses almost maximum value in the range of the averaged dynamic modification, virtually causing a dynamic enhancement of the electronic factor. Qualitatively, we can say that the range of the averaged dynamic modification is large for the system with a large degree of destructive interference. To describe it more concretely, we define the system's degree of destructive interference Q^s as follows

TABLE 2: Calculated Values of the Standard Deviation σ of log $|T_{DA}|$ and the Range of the Averaged Dynamic Modification D for the Six Kinds of Ru-Modified Azurins

derivative	σ	D	derivative	σ	D
His83	0.556	167	His122	0.550	158
His107	0.668	470	His124	0.519	119
His109	0.538	142	His126	0.591	231

$$\log Q^{s} \equiv \langle \log Q \rangle \tag{59}$$

Then, we can say that the range of the averaged dynamic modification is large for the system with the large value of Q^s. Among the six derivatives in Table 2, this relation between the range of the averaged dynamic modification and Q^s is not so much clearly seen because the range of the averaged dynamic modification is rather similar among them. However, according to our calculations for the electron transfer from Bph to Q_A in the reaction center, Q^s is small and the range of the averaged dynamic modification is also small (data not shown), supporting the above relation.

As we have already seen, T_{DA} changes its sign frequently because of the conformational fluctuation of protein media. Under such situation, it happens that $T_{DA} = 0$ holds true for certain conformations of protein media as we see in Figure 3. In this case, the tunneling current is blocked because of the complete interference among interatomic tunneling currents. This phenomenon can be called the multidimensional tunneling turn-off. If we can control the protein conformation in which T_{DA} becomes zero or nonzero, we can devise a switch of the electron tunneling current which works in less than 10 fs as we see in Figure 3.

Let us ask whether we can observe the effect of the degree of destructive interference experimentally. Consider the system that the degree of destructive interference Q distributes over considerable region because of the conformational fluctuation. In the case that conformations with a rather small value of Q appear frequently at room temperature, $\langle T_{DA}^2 \rangle$ is almost determined by those conformations with small value of Q, and its value will be nearly temperature independent in most cases. However, if the fluctuating conformations are confined to those with only small value of Q at low temperatures, $\langle T_{DA}^2 \rangle$ will be much increased at low temperatures. On the other hand, if the fluctuating conformations are confined to those with only large value of Q at low temperatures, $\langle T_{DA}^2 \rangle$ will be much decreased at low temperatures. With regard to this, recently, Skov et al. reported experimental data that the electron transfer rate of the Ru−His83 azurin is increased by about 3 times by lowering the temperature from 300 to 170 K.[55] This increase of the rate could not be explained by the temperature dependence of the Franck−Condon factor unless the vibrational quantum tunneling effect is applicable.[56] Therefore, we suggest that $\langle T_{DA}^2 \rangle$ is increased by about 3 times because of the confinement of the protein conformations with only small value of Q at 170 K, based on the above discussion.

In the other cases that conformations with a rather small value of Q appear only rarely at room temperature, $\langle T_{DA}^2 \rangle$ is almost determined by the conformations with both of small and large values of Q. When the temperature is lowered, the chance of the conformation with small value of Q being realized will be reduced, and so, $\langle T_{DA}^2 \rangle$ would be reduced. The above things are a qualitative picture of the temperature dependence of the electronic factor which fluctuates with time. To investigate the temperature dependence of the electron transfer rate quantitatively, however, we should first investigate the mechanism of the rapid fluctuation in Q and then carefully classify the factors which bears a property of temperature dependence. This is a future problem.

Recently, the role of the electronically nonadiabatic dynamics has been much studied for the electron transfer in the system that donor and acceptor are bridged by chemical bonds.[63−66] It appears that such a mechanism might be significant only for the system where donor−acceptor distance is rather small and rapid electron transfer takes place. Here, it should be mentioned that the dynamic effect of the protein media which we studied in this paper is describable within the Born−Oppenheimer scheme, and the nonadiabatic dynamics does not appear to work significantly.

Our method of the interatomic tunneling current was implemented so that we can visualize the electron tunneling route. The global feature of the interatomic tunneling current map looks similar to the pathway model[10,11] or tube model.[7,9] By taking the statistical average of the interatomic tunneling current on each plane j, we obtained an averaged tunneling route called the "worm model".[18] By taking into account the atom density involved in the worm, we plotted the logarithm of the electron tunneling rate as a function of the distance between donor and acceptor. We showed that this plot nicely coincides with the empirical relation recently obtained by the Dutton plot.[57] The isomorphism of the pathway model and the atomic density model presented by Dutton et al.[57] was also discussed by Jones et al.[58] recently. In connection with such studies, the present study will be situated as follows. Basically, a total of the interatomic tunneling current involves whole information of the electron tunneling phenomenon for a given system. Drawing the map of the interatomic tunneling currents is the most primitive way of using the original data. The calculation of the degree of destructive interference Q is the use of the interatomic tunneling currents by the intermediate level of average over the space by involving considerable amount of coherent information. The formation of the worm is made by the high level of average of the interatomic tunneling currents over the space. In such a way, we can derive any parameters related to the coherent tunneling property by a desired level of the average for the interatomic tunneling currents. The interatomic tunneling current method is indeed a promising one for the detailed study of the electron tunneling phenomena. The only problem here is that the interatomic tunneling currents through the protein are calculated by the extended Hückel method which is useful for the qualitative study. Therefore, it is desired to incorporate more advanced molecular orbital theory like HF level or density functional method[59−62,67] for the quantitative study. However, we think that the basic concept on the electron tunneling process obtained in this study will remain valid.

6. Conclusion

We examined the origin of the very rapid and large amplitude of fluctuation in the electron tunneling matrix element T_{DA} due to the thermal fluctuation of protein conformation. Then, we calculated T_{DA} by the extended Hückel level calculations combined with the MD simulations. We made analysis of the tunneling property by taking an intermediate level of average for the interatomic tunneling currents. Namely, we defined a new index, degree of the destructive interference Q. The index Q represents how many times the interatomic tunneling currents change their directions on the average in the course of the electron tunneling from donor to acceptor. An empirical relation that $|T_{DA}|$ is proportional to Q^{-1} holds true in the range of more than 2 orders of magnitude of Q. Drawing the interatomic tunneling currents maps for the different value of Q, we found that the tunneling current flows smoothly in the case of small Q but the tunneling current flows circularly and drops in the other part from the main route in the case of large Q. Therefore, we conclude that the very rapid and large amplitude (about 2 orders of magnitude) of fluctuation in T_{DA} is caused by the reconnection and the change in the direction of interatomic tunneling currents with considerable amplitude. In the case that

the system's degree of destructive interference is large (case of large Q^s), this dynamic behavior contributes to greatly enhance the electron transfer rate. A large scale of variation in the electron tunneling matrix element T_{DA} due to the thermal fluctuation of protein conformation provides us a nice opportunity for investigating an essential role of the coherent property in the long-range electron transfer through protein media which was not noticed before. We suggested that the phonon-modified tunneling effect would not significantly appear in the nuclear factor but appear substantially in the electronic factor. We also pointed out a possibility that a variety of temperature dependences of the electronic factor will be realized through the modification of the large fluctuation in Q by changing the temperature. The present study is just one step toward this fascinating problem.

Acknowledgment. The authors are grateful to Prof. D. N. Beratan in Duke University for invaluable discussion on the temperature dependence of the electronic factor. This work was supported by the Grant-in-Aid on Scientific Research on Priority Area "Molecular Physical Chemistry" No. 11166230 to T. K. from the Ministry of Education, Culture, Sports, Science and Technology of Japan. This work was also supported by Grant-in-Aid for Scientific Research on Priority Areas (C) "Genome Information Science" to T. Y. from the Ministry and Education, Culture, Sports, Science and Technology of Japan.

Appendix A

Here, we derive basic equations of the electron tunneling currents eqs 35−37 by a little different method from Stuchebrukhov.[19−22]

An electron density P at certain electronic state Ψ is given as follows:

$$P = \langle\Psi|\Psi\rangle \tag{A1}$$

where Ψ is a vector of the electronic state. Its component ψ is written by a molecular orbital method as

$$\psi = \sum_{\mu} C_{\nu}\phi_{\nu} \tag{A2}$$

where ϕ_{ν} means the atomic orbital. Using these notations, the electron density P_{μ} at the atomic orbital ϕ_{μ} is obtained as follows:

$$P_{\mu} = C_{\mu}^{*}\langle\phi_{\mu}|\Psi\rangle = \sum_{\nu} C_{\mu}^{*}C_{\nu}S_{\mu\nu} \tag{A3}$$

where $S_{\mu\nu}$ is the overlap integral between the atomic orbitals ϕ_{μ} and ϕ_{ν}.

Now, we adopt the 2-state model for the electron transfer system. The 2-state Hamiltonian is written as follows:

$$H = \begin{pmatrix} \hat{H}^{D} & \hat{T}^{DA} \\ \hat{T}^{AD} & \hat{H}^{A} \end{pmatrix} \tag{A4}$$

where D and A mean the states in which electron localizes in the donor and acceptor, respectively. The nondiagonal components satisfy $\hat{T}^{DA} = \hat{T}^{AD*}$ and it is expressed as

$$\hat{T}^{DA} = \hat{H} - E\hat{I} \tag{A5}$$

where $\hat{I}$ is a unit matrix. the electronic state Ψ is written by the initial state ψ^{i} and final state ψ^{f} as follows:

$$\Psi = \begin{pmatrix} \psi^{i}(t) \\ \psi^{f}(t) \end{pmatrix} = \begin{pmatrix} \cos(\omega t)\psi_0^{i} \\ i\sin(\omega t)\psi_0^{f} \end{pmatrix} \tag{A6}$$

where the angular frequency ω is defined as $T_{DA}/\hbar$. The initial and final states are given by the same way as eqs 7 and 8

$$\psi_0^{i} = \sum_{\nu} C_{\nu}^{i}\phi_{\nu} \tag{A7}$$

$$\psi_0^{f} = \sum_{\nu} C_{\nu}^{f}\phi_{\nu} \tag{A8}$$

Now, the Schrödinger equation for the electron density P is given as follows:

$$i\hbar\frac{\partial P}{\partial t} = i\hbar\frac{\partial\langle\Psi|\Psi\rangle}{\partial t} = i\hbar\frac{\partial\langle\Psi|}{\partial t}|\Psi\rangle + i\hbar\langle\Psi|\frac{\partial|\Psi\rangle}{\partial t} = -\langle\Psi|H|\Psi\rangle^{*} + \langle\Psi|H|\Psi\rangle = 2i_{Im}(\langle\Psi|H|\Psi\rangle) \tag{A9}$$

Substituting eqs A6, A7, and A8 into the 2-state Hamiltonian eq A4, we obtain

$$\langle\Psi|H|\Psi\rangle = \langle\psi_0^{i}|\hat{H}^{D}|\psi_0^{i}\rangle\cos^2(\omega t) + \langle\psi_0^{f}|\hat{H}^{A}|\psi_0^{f}\rangle\sin^2(\omega t) + i(\langle\psi_0^{i}|\hat{T}^{DA}|\psi_0^{f}\rangle - \langle\psi_0^{f}|\hat{T}^{AD}|\psi_0^{i}\rangle)\sin(\omega t)\cos(\omega t) \tag{A10}$$

Substituting eq A10 into the Schrödinger equation eq A9, we obtain

$$\frac{\partial P}{\partial t} = \frac{1}{\hbar}(\langle\psi_0^{i}|\hat{T}^{DA}|\psi_0^{f}\rangle - \langle\psi_0^{f}|\hat{T}^{AD}|\psi_0^{i}\rangle)\sin(2\omega t) \tag{A11}$$

The density P_{μ} of the atomic orbital μ is obtained by the same way. By comparing eq A1 with eqs A3 and A11, we obtain the following equation:

$$\frac{\partial P_{\mu}}{\partial t} = \frac{1}{\hbar}(C_{\mu}^{i*}\langle\phi_{\mu}|\hat{T}^{DA}|\psi_0^{f}\rangle - C_{\mu}^{f*}\langle\phi_{\mu}|\hat{T}^{AD}|\psi_0^{i}\rangle)\sin(2\omega t) \tag{A12}$$

Substituting eqs A7 and A8 into eq A12, we obtain

$$\frac{\partial P_{\mu}}{\partial t} = \frac{1}{\hbar}\sum_{\nu}(C_{\mu}^{i*}C_{\nu}^{f}\langle\phi_{\mu}|\hat{T}^{DA}|\phi_{\nu}\rangle - C_{\mu}^{f*}C_{\nu}^{i}\langle\phi_{\mu}|\hat{T}^{AD}|\phi_{\nu}\rangle)\sin(2\omega t) \tag{A13}$$

Substituting eq A5 into eq A13 and assuming that C_{μ}^{i}, C_{μ}^{f}, $H_{\mu\nu}$, and $S_{\mu\nu}$ have real values, we obtain

$$\frac{\partial P_{\mu}}{\partial t} = \frac{1}{\hbar}\sum_{\nu}(C_{\mu}^{i}C_{\nu}^{f} - C_{\mu}^{f}C_{\nu}^{i})(H_{\mu\nu} - ES_{\mu\nu})\sin(2\omega t) \tag{A14}$$

We make use of the continuity property of the tunneling currents.[19−21] When the tunneling current from the μth orbital to the νth orbital is written as $J_{\mu\nu}(t)$, the electron density P_{μ} is related to them as follows:

$$\frac{\partial P_{\mu}}{\partial t} = \sum_{\nu} J_{\mu\nu}(t) \tag{A15}$$

Comparing eq A14 with eq A15, the tunneling current $J_{\mu\nu}(t)$ is obtained as

$$J_{\mu\nu}(t) = \frac{1}{\hbar}(C_{\mu}^{i}C_{\nu}^{f} - C_{\mu}^{f}C_{\nu}^{i})(H_{\mu\nu} - ES_{\mu\nu})\sin(2\omega t) \tag{A16}$$

The time-dependent part $\sin(2\omega t)$ is common to all of the tunneling currents. Then, we use the part of the time-independent tunneling current:

$$J_{\mu\nu} = \frac{1}{\hbar}(C_\mu^{\mathrm{i}} C_\nu^{\mathrm{f}} - C_\mu^{\mathrm{f}} C_\nu^{\mathrm{i}})(H_{\mu\nu} - ES_{\mu\nu}) \qquad \text{(A17)}$$

An interatomic tunneling current is obtained as follows:

$$J_{\mathrm{ab}} = \sum_{\mu\in a,\nu\in b} J_{\mu\nu} \qquad \text{(A18)}$$

where *a* and *b* mean specific atoms. The electron tunneling matrix element T_{DA} is expressed by using this interatomic tunneling current as follows:[17−21]

$$\sum_{a\in\Omega_{\mathrm{D}}^j, b\notin\Omega_{\mathrm{D}}^j} J_{\mathrm{ab}} = \frac{1}{\hbar} T_{\mathrm{DA}} \qquad \text{(A19)}$$

where Ω_{D}^j is a region of the donor side from the plane *j* placed perpendicularly to the line connecting a donor and acceptor. In this case, the value of the sum in eq A19 is independent of the position of plane.

References and Notes

(1) Marcus, R. A.; Sutin, N. *Biochim. Biophys. Acta* **1985**, *811*, 265.
(2) Daizadeh, I.; Medvedev, E. S.; Stuchebrukhov, A. A. *Proc. Natl. Acad. Sci. U.S.A.* **1997**, *94*, 3703.
(3) Antony, J.; Medvedev, D. M.; Stuchebrukhov, A. A. *J. Am. Chem. Soc.* **2000**, *122*, 1057.
(4) Wolfgang, J.; Risser, S. M.; Priyadarshy, S.; Beratan, D. N. *J. Phys. Chem. B* **1997**, *101*, 2986.
(5) Aquino, A. J. A.; Beroza, P.; Reagan, J. J.; Onuchic, J. N. *Chem. Phys. Lett.* **1997**, *275*, 181.
(6) Balabin, I. A.; Onuchic, J. N. *Science* **2000**, *290*, 114.
(7) Regan, J. J.; Bilio, A. J. D.; Langen, R.; Skov, L. K.; Winkler, J. R.; Gray, H. B.; Onuchic, J. N. *Chem. Biol.* **1995**, *2*, 489.
(8) Regan, J. J.; Onuchic, J. N.; *Electron Transfer: From Isolated Molecules to Biomolecules, Part Two*; Jortner, J., Bixon, M., Eds.; John Wiley & Sons: New York, 1999; p 467.
(9) de Andrade, P. C. P.; Onuchic, J. N. *J. Chem. Phys.* **1998**, *108*, 4292.
(10) Beratan, D. N.; Onuchic, J. N.; Hopfield, J. J. *J. Chem. Phys.* **1987**, *86*, 4488.
(11) Onuchic, J. N.; Beratan, D. N.; Winkler, J. R.; Gray, H. B. *Annu. Rev. Biophys. Biomol. Struct.* **1992**, *21*, 349.
(12) Balabin, I. A.; Onuchic, J. N. *J. Phys. Chem.* **1996**, *100*, 11573.
(13) Paddon-Row, M. N. In *Electron Transfer in Chemistry*; Blzani, V., Ed.; Wiley-VCH: New York, 2000; Vol. 3, 179.
(14) Paddon-Row: M. N. *Acc. Chem. Res.* **1994**, *27*, 18.
(15) Oliver, A. M.; Craig, D. C.; Paddon-Row, M. N.; Kroon, J.; Verhoeven, J. W. *Chem. Phys. Lett.* **1988**, *150*, 366.
(16) Jones, G. A.; Paddon-Row, M. N.; Carpenter, B. K.; Piotrowiak, P. *J. Phys. Chem. A* **2002**, *106*, 5011.
(17) Kawatsu, T.; Kakitani, T.; Yamato, T. *Inorg. Chim. Acta* **2000**, *300−302*, 862.
(18) Kawatsu, T.; Kakitani, T.; Yamato, T. *J. Phys. Chem. B* **2001**, *105*, 4424.
(19) Stuchebrukhov, A. A. *J. Chem. Phys.* **1996**, *105*, 10819.
(20) Stuchebrukhov, A. A. *J. Chem. Phys.* **1997**, *107*, 6495.
(21) Stuchebrukhov, A. A. *J. Chem. Phys.* **1996**, *104*, 8424.
(22) Cheung, M. S.; Daizadeh, I.; Stuchebrukhov, A. A.; Heelis, P. F. *Biophys. J.* **1999**, *76*, 1241.
(23) Larsson, S. *J. Am. Chem. Soc.* **1981**, *103*, 4034.
(24) Larsson, S. *Chem. Phys. Lett.* **1982**, *90*, 136.
(25) Kawatsu, T.; Kakitani, T.; Yamato, T. *J. Phys. Chem. B* **2002**, *106*, 5068.
(26) Katz, D. J.; Stuchebrukhov, A. A. *J. Chem. Phys.* **1998**, *109*, 4960.
(27) Priyadarshy, S.; Skourtis, S. S.; Risser, S. M.; Beratan, D. N. *J. Chem. Phys.* **1996**, *104*, 9473.
(28) Siddarth, P.; Marcus, R. A. *J. Phys. Chem.* **1990**, *94*, 8430.
(29) Siddarth, P.; Marcus, R. A. *J. Phys. Chem.* **1993**, *97*, 2440.
(30) Siddarth, P.; Marcus, R. A. *J. Phys. Chem.* **1993**, *97*, 6111.
(31) Siddarth, P.; Marcus, R. A. *J. Phys. Chem.* **1993**, *97*, 13078.
(32) Stuchebrukhov, A. A. *Chem. Phys. Lett.* **1997**, *265*, 643.
(33) Daizadeh, I.; Gehlen, J. N.; Stuchebrukhov, A. A. *J. Chem. Phys.* **1997**, *106*, 5658.
(34) Stuchebrukhov, A. A. *Chem. Phys. Lett.* **1994**, *225*, 55.
(35) Stuchebrukhov, A. A.; Marcus, R. A. *J. Phys. Chem.* **1995**, *99*, 7581.
(36) Gehlen, J. N.; Daizadeh, I.; Stuchebrukhov, A. A.; Marcus, R. A. *Inorg. Chim. Acta* **1996**, *243*, 271.
(37) Larsson, S. *J. Biol. Inorg. Chem.* **2000**, *5*, 560.
(38) Saito, M. *Mol. Simul.* **1992**, *8*, 321.
(39) Morikami, K.; Nakai, T.; Kidera, A.; Saito, M.; Nakamura, H. *Comput. Chem.* **1992**, *16*, 243. PRESTO (A vectorized molecular mechanics program for biopolymers).
(40) Cornell, W. D.; Cieplak, P.; Bayly, C. I.; Gould, I. R.; Merz, K. M., Jr.; Ferguson, D. M.; Spellmeyer, D. C.; Fox, T.; Caldwell, J. W.; Kollman, P. A. *J. Am. Chem. Soc.* **1995**, *117*, 5179.
(41) Geremia, S.; Calligaris, M. *J. Chem. Soc., Dalton Trans.* **1997**, 1541.
(42) Ungar, L. W.; Scherer, N. F.; Voth, G. A. *Biophys. J.* **1997**, *72*, 5.
(43) Wuttke, D. S.; Bjerrum, M. J.; Winkler, J. R.; Gray, H. B. *Science* **1992**, *256*, 1007.
(44) Casimiro, D. R.; Richards, J. H.; Winkler, J. R.; Gray, H. B. *J. Phys. Chem.* **1993**, *97*, 13073.
(45) Langen, R.; Chang, I.-J.; Germanas, J. P.; Richard, J. H.; Winkler, J. R.; Gray, H. B. *Science* **1995**, *268*, 1733.
(46) Gray, H. B.; Winkler, J. R. *Annu. Rev. Biochem.* **1996**, *65*, 537.
(47) Bonander, N.; Vänngård, T.; Tsai, L.-C.; Langer, V.; Nar, H.; Sjölin, L. *Proteins* **1997**, *27*, 385.
(48) Adman, E. T.; Jensen, L. H. *Isr. J. Chem.* **1981**, *21*, 8.
(49) Adman, E. T.; Stenkamp, R. E.; Sieker, L. C.; Jensen, L. H. *J. Mol. Biol.* **1978**, *124*, 35.
(50) Reddy, K. B.; Cho, M.-o. P.; Wishart, J. F.; Emge, T. J.; Isied, S. S. *Inorg. Chem.* **1996**, *35*, 7241.
(51) Howell, J.; Rossi, A.; Wallace, D.; Haraki, K.; Hoffmann, R. *QCPE* **1977**, *11*, 344. FORTICON8 (Extend Hükel method program).
(52) Vela, A.; Gázquez, J. L. *J. Phys. Chem.* **1988**, *92*, 5688.
(53) Kincaid, D. R.; Respess, J. R.; Young, D. M.; Grimes, R. G. *ITPACK 2C*; University of Texas: Austin, TX, 1999 (A fortran package for solving large sparse linear system by adaptive accelerated iterative methods).
(54) Marcus, R. A. *J. Chem. Phys.* **1956**, *24*, 966, 979.
(55) Skov, L. K.; Pascher, T.; Winkler, J. R.; Gray, H. B. *J. Am. Chem. Soc.* **1998**, *120*, 1102.
(56) Brunschwig, B. S.; Logan, J.; Newton, M. D.; Sutin, N. *J. Am. Chem. Soc.* **1980**, *102*, 5798.
(57) Page, C. C.; Moser, C. C.; Chen, X.; Dutton, P. L. *Nature* **1999**, *402*, 47.
(58) Jones, M. L.; Kurnikov, I. V.; Beratan, D. N. *J. Phys. Chem. A* **2002**, *2002*, 106.
(59) Stuchebrukhov, A. A. *J. Chem. Phys.* **1998**, *108*, 8499.
(60) Stuchebrukhov, A. A. *J. Chem. Phys.* **1998**, *108*, 8510.
(61) Daizadeh, I.; Guo, J.-x.; Stuchebrukhov, A. A. *J. Chem. Phys.* **1999**, *108*, 8865.
(62) Stuchebrukhov, A. A. *Int. J. Quantum Chem.* **2000**, *77*, 16.
(63) Kendrick, B. K.; Mead, C. A.; Truhlar, D. G. *Chem. Phys.* **2002**, *277*, 31.
(64) Hack, M. D.; Wensmann, A. M.; Truhlar, D. G. *J. Chem. Phys.* **2001**, *115*, 1172.
(65) Volobuev, Y. L.; Hack, M. D.; Topaler, M. S.; Truhlar, D. G. *J. Chem. Phys.* **2000**, *112*, 9716.
(66) Klimkāns, A.; Larson, S. *Int. J. Quantum Chem.* **2000**, *77*, 211.
(67) Prezhdo, O. V.; Kindt, J. T.; Tully, J. C. *J. Chem. Phys.* **1999**, *111*, 7818.